Journal of Sound and Vibration (2000) **237**(2), 319–335
doi:10.1006/jsvi.2000.3058, available online at http://www.idealibrary.com on IDEAL®

VIBRATION AND STABILITY OF A CRACKED TRANSLATING BEAM

KEVIN D. MURPHY AND YIN ZHANG

Department of Mechanical Engineering, University of Connecticut, Storrs, CT 06269-3139, *U.S.A.*

(*Received* 10 *December* 1999, *and in final form* 30 *March* 2000)

The vibration and stability characteristics of a cracked beam translating between fixed supports are investigated. Using Hamilton's principle and elementary fracture mechanics, the equations of motion for the beam are developed. Throughout this analysis it is assumed that the crack is shallow and always remains open, i.e., crack closure and the associated impact conditions are not considered. In order to restrict attention to the open crack scenario, parameter regimes corresponding to (1) a fully open crack, (2) a fully closed crack, and (3) a partly open–partly closed crack are clearly identified. For parameter values in regime (1), the free vibration characteristics are studied via an eigenanalysis. This shows that the natural frequencies ($\mathrm{Im}(\lambda)$) and stability characteristics ($\mathrm{Re}(\lambda)$) fluctuate as the crack translates along with the beam between the two supports. For the shallow cracks being considered, the fluctuations are attributed primarily to the localized drop in the mass per unit length (occurring at the crack) rather than from the increased flexibility. Furthermore, the magnitudes of these fluctuations are shown to vary with both the axial transport speed and the crack depth and are mapped in the control parameter space. Implications for the free and forced vibration problems are discussed.

1. INTRODUCTION

Axially moving strings, cables, beams, and webs have been widely studied in the literature [1, 2] and deal with applications including composite fiber threadlines, bandsaws, and paper manufacturing. The present study considers the influence of a shallow crack on the vibration and stability characteristics of a translating beam. In particular, the system consists of a flexible beam translating along its longitudinal axis at a constant speed c between two pin supports, which are fixed in inertial space. The beam also possesses a single crack of fixed depth, which translates with the beam. Throughout this work, it is assumed that the applied axial tension is large and that the internal bending moment is small (a reasonable assumption for small amplitude, linear motion) such that the crack always remains open. In other words, impacting conditions associated with crack closure are not considered [3, 4]. To assure the validity of this assumption, as analysis is presented which divides the applied axial tension—internal bending moment parameter plane into regions corresponding to (1) a completely open crack, (2) a completely closed crack, and (3) a partly open–partly closed crack. Then the attention is focused on the behavior in the *always open* regime.

Introduction of a crack into a structure produces two significant effects. First, there is a change in the stress field near the crack trip which increases the local flexibility. Numerous studies have used the stress intensity factor (K_I) to characterize this change in flexibility; see

0022-460X/00/420319 + 17 $35.00/0

reference [5]. The expressions for K_I have been commonly used to investigate the vibration characteristics of systems, including (non-translating) cracked beams, rotors, and plates [6–10]. Still others have used a variational technique with exponential "crack functions" to obtain a consistent theoretical description of the problem [11–13].

The second effect, which is not commonly incorporated, involves the discontinuity in the mass per unit length of the beam produced by the presence of the crack. In a related study, Wickert and Mote [14] examined the dynamics of a translating string carrying a discrete mass (as opposed to a discrete material void). They showed that the mass acted to scatter harmonic waves and that the frequencies fluctuated as the mass location varied during translation.

In the present study, both effects are incorporated into a mathematical model to describe the linear vibrations (both axial and transverse) of a cracked, translating beam. The governing PDEs are discretized to a set of ODEs and then, using a shallow crack assumption, they are linearized about the straight equilibrium configuration. The vibration and stability characteristics are examined using an eigenvalue analysis. It is shown that, like the results presented in reference [14], the natural frequencies ($\mathrm{Im}\,\lambda$) and the stability characteristics ($\mathrm{Re}\,\lambda$) fluctuate as the crack location moves. Furthermore, the influences of the transport speed and the crack depth on the amplitude of these fluctuations are demonstrated. The implications of these results for both the free and forced response are considered and discussed.

2. MODEL DEVELOPMENT

2.1. SOME USEFUL CONCEPTS FROM FRACTURE MECHANICS

To begin, consider Figure 1; this shows a crack in a linearly elastic material. Points in the material are identified by the polar co-ordinates r and θ, centered at the crack tip. It is well established that the stress field associated with a crack decays as $1/\sqrt{r}$ and varies with θ [15]. This is usually expressed in the form

$$\sigma_{ij} = \frac{K_I}{\sqrt{r}} f_{ij}(\theta),$$

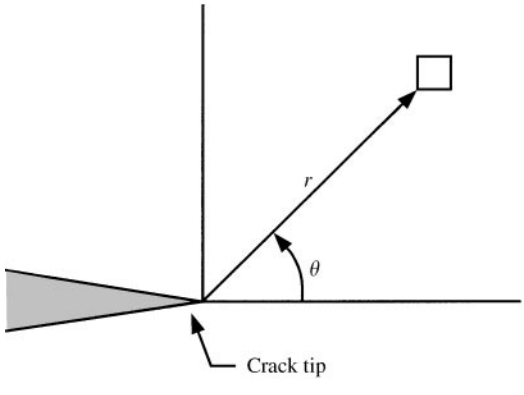

Figure 1. Geometry and polar co-ordinate system used to describe the stress field near a crack tip.

where K_I is the stress intensity factor and is a function of the applied load and the size or depth of the crack. If a combined load is applied, the resultant stress is simply the sum of the individual stresses since the system is linear. For this study, the primary focus is on combined bending and axial stretching of a long, thin beam. In this case, shear is ignored and the net axial stress is

$$\sigma = \sigma^b + \sigma^s = \frac{1}{\sqrt{\pi r}}[K_I^b f_b(\theta) + K_I^s f_s(\theta)]. \tag{1}$$

If the crack is allowed to propagate, new surface area is continually generated. This disruption of the continuum requires that some of the internal strain energy of the material be dissipated. This converted energy is usually described in terms of an energy release rate, G. Of course, the amount of energy dissipated depends on *how* the crack is propagated. Typically, cracks propagate in one of the three ways: mode I—crack opening, mode II—sliding (in-plane shear), and mode III—tearing (anti-plane shear); see reference [15]. For the remainder of this study, only mode I deformations will be considered.

Under a bending/stretching loading scenario, the strain energy may be expressed in terms of the square of the axial stress. Given equation (1), coupling occurs between the bending and stretching terms. However, unlike the classic Kirchhoff beam theory, this coupling remains after the infinitesimal energy dU is integrated over the domain. In other words, $U \propto [K_I^b + K_I^s]^2$. Because the energy released during crack propagation is simply a conversion of the strain energy, it should not be surprising that G is also proportional to squared sum of the stress intensity factors. The particular expression for the energy release rate for plane strain problems is presented in reference [15] and takes the form

$$G(a/b) = \frac{1 - \nu^2}{E}(K_I^b + K_I^s)^2, \tag{2}$$

where the stress intensity factors are functions of the non-dimensional crack depth a/b and are given in reference [5]. This expression for the energy release rate will be used in the following section to obtain the change in compliance due to a crack for a tensioned beam undergoing transverse and axial vibrations.

2.2. THE EFFECT OF A CRACK ON THE LOCAL STIFFNESS

A schematic of the cracked beam under consideration is shown in Figure 2(a). The system consists of two pin supports fixed in inertial space, which support the beam. The beam has length L, height b, cross-sectional area A, axial transport speed c (moving to the right, as shown), and is subjected to a constant tension force P. It also has a crack of fixed depth a that translates with the beam. The crack location changes constantly and is given by the variable $\xi_0 = x_0/L$. The presence of the crack reduces the stiffness of the beam both in axial stretching and in bending. In other words, a given load will produce more deformation in the cracked beam than in its uncracked counterpart. This additional deformation is highly localized near the crack and not distributed evenly over the structure. The asymmetric crack also causes the neutral axis to dip down from the centerline in the vicinity of the crack. This is shown schematically with a dashed line in Figure 2(a). This asymmetry produces an eccentric loading scenario which leads to coupling between the bending and the stretching deformations.

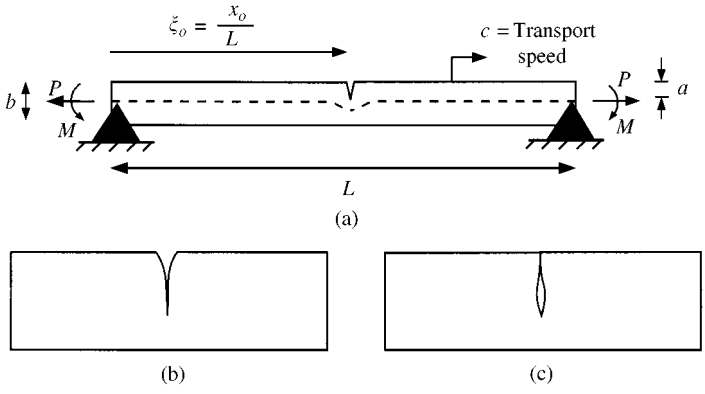

Figure 2. (a) A schematic of the cracked translating beam. (b) Crack closure beginning at the crack tip. (c) Crack closure beginning at the crack mouth.

To begin, consider the *net* effect of the crack and forget, for the moment, that the additional deformation is highly localized. In this case, the global force–deformation relations are

$$\begin{Bmatrix} d \\ \theta \end{Bmatrix} = [C] \begin{Bmatrix} P_1 \\ P_2 \end{Bmatrix}, \tag{3}$$

where d and θ are measured of the overall (global) axial and rotational deformations, respectively, $P_1 = P$ is the axial tension, $P_2 = M$ is the bending moment, and $[C]$ is the compliance matrix. In the absence of a crack, the compliance matrix is diagonal with terms $c_{11} = (L/AE)_0$ and $c_{22} = (L/EI)_0$, where the subscript indicates that this refers to the uncracked structure. The addition of the crack increases the diagonal elements and introduces off-diagonal terms coupling the axial and the bending deformations:

$$[C] = \begin{bmatrix} \left(\frac{L}{EA}\right)_0 + \Delta c_{11} & \Delta c_{12} \\ \Delta c_{12} & \left(\frac{L}{EA}\right)_0 + \Delta c_{22} \end{bmatrix}, \tag{4}$$

where Δc_{ij} is the change in flexibility which leads to the net increase in the global deformation variables. The appropriate expression for the change in flexibility is

$$\Delta c_{ij} = \frac{\partial^2}{\partial P_i \partial P_j} \int_0^a G(\bar{a})\, \mathrm{d}\bar{a}, \tag{5}$$

where a is the depth of the crack, G is the elastic energy release rate, and P_i are the generalized forces described previously. A derivation of equation (5) is presented in Appendix A. It should be noted that this description of the compliance matrix is only valid for situations where the crack remains open. If the crack should close, the compliance will experience a discontinuity (a strong non-linearity) and a very different analysis would be required. The limitations and applicability of the present open-crack theory are discussed in section 2.3.

The global change in compliance may be computed using equations (2) and (5) along with the expressions for the stress intensity factors for a beam with an edge crack in bending and stretching. These are found in reference [5] and take the form

$$K_I^s = \frac{P}{bt}\sqrt{\pi a}\,F_1(a/b), \qquad K_I^b = \frac{6M}{b^2 t}\sqrt{\pi a}\,F_2(a/b), \tag{6, 7}$$

where $F_1(a/b)$ and $F_2(a/b)$ are

$$F_1(a/b) = \sqrt{\frac{2b}{\pi a}\tan\left(\frac{\pi a}{2b}\right)}\,\frac{0{\cdot}752 + 2{\cdot}02(a/b) + 0{\cdot}37(1 - \sin(\pi a/2b))^3}{\cos(\pi a/2b)}, \tag{8}$$

$$F_2(a/b) = \sqrt{\frac{2b}{\pi a}\tan\left(\frac{\pi a}{2b}\right)}\,\frac{0{\cdot}923 + 0{\cdot}1999(1 - \sin(\pi a/2b))^4}{\cos(\pi a/2b)}. \tag{9}$$

From this formulation, the global stiffness matrix may be computed by simply inverting the flexibility matrix, equation (4).

Thus far, a global approach has been taken despite the fact that the additional deformation is known to be localized near the crack. This approach was taken because the expression for the change in compliance, equation (5), was defined using the global deformations d and θ. To transform this global approach into a local one, two steps are taken. First, the deformation measures are changed to the local measures of "stretching" strain and curvature. In other words, d and θ are replaced by $\varepsilon_s(x)$ and $\kappa(x)$ respectively. As a result, the stiffness is multiplied by L. To localize the additional deformation, the changes in the stiffness, ΔK_{ij}, are multiplied by L and the Dirac delta function centered at the location of the crack, x_0. This produces the stiffness matrix

$$[K] = \begin{bmatrix} (EA)_0 - \Delta K_{11} L\delta(x - x_0) & \Delta K_{12} L\delta(x - x_0) \\ \Delta K_{12} L\delta(x - x_0) & (EI)_0 - \Delta K_{22} L\delta(x - x_0) \end{bmatrix}, \tag{10}$$

where the ΔK_{ij} may be computed by inverting both the uncracked global compliance matrix and the cracked global compliance matrix (equation (4)) and subtracting the former from the latter.

2.3. LIMITATIONS

To this point, the discussion has focused on the open-crack scenario. In other words, crack closure and the associated discontinuity in the stiffness have not been considered. But under what circumstances is this a reasonable assumption? To build some physical insight, first consider the static case. If the beam is subjected to a tensile load and a positive bending moment, the crack will always remain open; see Figure 2(a). Conversely, a compressive load and a negative bending moment will lead to a completely closed crack. If the sign of the axial load and the moment are opposite, the status of the crack will depend on the relative magnitudes of the loads and the result is not immediately obvious. This is the underlying difficulty in the dynamic problem since the beam vibration causes the internal bending moment to periodically change sign. The objective here is to determine what combinations of the constant axial tension and the bending moment lead to the initiation of crack closure.

The initiation of closure may begin either at the crack tip or mouth, as shown schematically in Figures 2(b) and 2(c). For the moment, focus on the crack tip closing

scenario is shown in Figure 2(b). From linear elasticity, it has been shown that the displacement field near the crack tip follows a $\sqrt{r}$ law where r is the distance from the crack tip along the crack [15]. Specifically, $u(r) = (K_I/E)(8r/\pi)^{1/2}$, where the stress intensity factor is the sum of the stress intensity factors for bending and stretching: $K_I = K_I^b + K_I^s$. Using this expression along with equations (6)–(9), the crack tip opening is described by

$$u(r) = \left[\frac{6M}{b} F_b(a/b) + PF_s(a/b)\right] \frac{\sqrt{\pi a}}{bE} \left(\frac{8r}{\pi}\right)^{1/2}. \tag{11}$$

As the crack tip begins to close, the displacement field of the crack drops to zero even for non-zero r. As a result, the crack tip closure criterion is found by setting the coefficient in equation (11) equal to zero. This yields

$$\frac{M}{Eb^3} = \frac{P}{Eb^2}\left[\frac{0{\cdot}923 + 0{\cdot}199(1 - \sin((\pi/2)\,a/b))^4}{6(0{\cdot}752 + 2{\cdot}02(a/b) + 0{\cdot}37(1 - \sin((\pi/2)\,a/b))^3)}\right], \tag{12}$$

which is a straight line in the (P, M) parameter plane.

Next, consider the crack mouth closing scenario, as shown in Figure 2(c). Crack closure begins when the mouth displacement due to bending is equal and opposite to the mouth displacement due to stretching. In other words, $\delta_b + \delta_s = 0$. Using the expressions presented in reference [5] for the mouth deflections, the criterion for mouth closure is

$$\frac{M}{Eb^3} = \frac{P}{Eb^2}\left[\frac{1{\cdot}46 + 3{\cdot}42(1 - \cos((\pi/2)\,a/b))}{6\cos^2((\pi/2)\,a/b)(0{\cdot}8 - 1{\cdot}7(a/b) + 2{\cdot}4\,(a/b)^2 + 0{\cdot}66/(1 - a/b)^2}\right]. \tag{13}$$

This is also a straight line in the (P, M) parameter plane.

Equations (12) and (13) are shown in Figure 3 with a solid and dashed line, respectively. This is for a crack depth of $a/b = 0{\cdot}3$. As indicated, the combination of a tensile load ($P > 0$) and a positive bending moment ($M > 0$) leads to an open crack. Similarly, a compressive

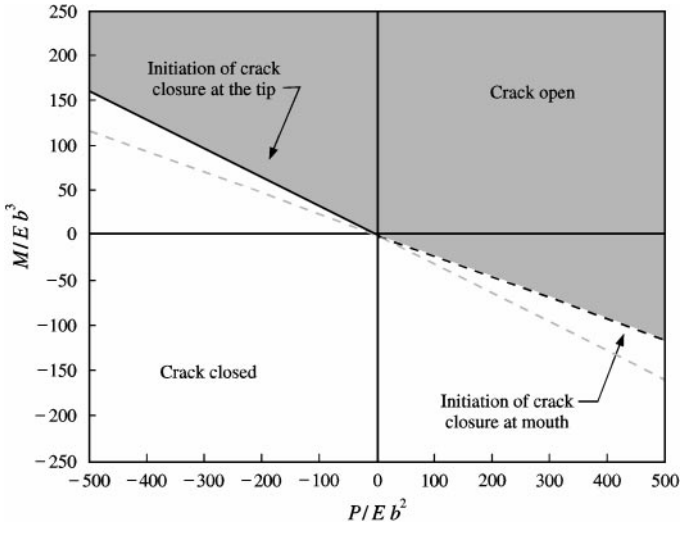

Figure 3. The (P, M) parameter plane showing various types of behavior including a completely open crack, a completely closed crack, and the onset of crack closure (either at the crack tip or mouth).

load ($P < 0$) and a negative bending moment ($M < 0$) will ensure a closed crack. However, the second and fourth quadrants of this figure are more complicated because they contain the parameter combinations which initiate crack closure. Fortunately, because this work deals with open cracks, only the transition from an open crack to the initiation of closure is critical. The *initiation of closure* lines have been darkened in Figure 3. It is also worth mentioning that under a tensile (compressive) load the crack will always begin to close at the mouth (tip).

As discussed previously, the objective of this work is to focus on the dynamics of a translating beam containing an open crack. For the results of this work to remain valid, the amplitude of the bending moment must satisfy

$$\left|\frac{M}{Eb^3}\right| < \left|\frac{P}{Eb^2}\left[\frac{1{\cdot}46 + 3{\cdot}42(1 - \cos((\pi/2)\,a/b))}{6\cos^2((\pi/2)\,a/b)(0{\cdot}8 - 1{\cdot}7(a/b) + 2{\cdot}4\,(a/b)^2 + 0{\cdot}66/(1 - a/b)^2}\right]\right|, \tag{14}$$

where P is the specified axial load.

2.4. EQUATIONS OF MOTION

Hamilton's principle is used to obtain the equations of motion for this system. As a result, expressions for the internal strain energy, the kinetic energy, and the external work must be developed.

The strain energy of the beam may be written as

$$U = \int_0^L \frac{1}{2}\,\mathbf{q}^{\mathrm{t}}[K]\mathbf{q}\,\mathrm{d}x, \tag{15}$$

where U is the strain energy, $[K]$ is the stiffness matrix defined by equation (10), and $\mathbf{q}^{\mathrm{t}} = \{\varepsilon_s, \kappa\}$ is a generalized deformation vector. Under the typical small slope assumption the curvature is simplified to $\kappa = v_{,xx}$. Also, ε_s is the stretching strain which is expressed as $\varepsilon_s = (u_{,x} + P/EA)$. The last term in this expression, P/EA, represents a static strain resulting from the constant axial load P.

Under the assumption that the crack is shallow and that the beam is long and thin, the coupling terms are extremely small and may be neglected. This can be shown by examining the static equilibrium equations

$$P = K_{11}u_{,x} + K_{12}\kappa, \qquad M = K_{21}u_{,x} + K_{22}\kappa. \tag{16}$$

Consider fixing the axial tension and choosing the most extreme bending moment permitted (see equation (13)). Under this loading situation, the equilibrium equations may be solved for the deformations and the relative contributions of the coupling terms, $K_{12}\kappa/P$ and $K_{21}u_{,x}/M$, may then be assessed. The results of such an analysis are presented in Tables 1(a) and 1(b). In each case, these coupling terms are all less than 3% even for a moderate crack ($a/b = 0{\cdot}4$) and an extremely stocky beam ($b/L = 0{\cdot}1$).

Eliminating the off-diagonal terms leads to the following expression for the strain energy:

$$U = \int_0^L \left[\frac{1}{2}\,EIv_{,xx}^2 + \frac{1}{2}\,EA\left(u_{,x} + \frac{P}{EA}\right)^2\right]\mathrm{d}x, \tag{17}$$

where $EI = (EI)_0 - \Delta K_{11}L\delta(x - x_0)$, $EA = (EA)_0 - \Delta K_{22}L\delta(x - x_0)$, x_0 refers to the location of the crack, and the ΔK_{ij} are computed using the methods described in section 2.2.

TABLE 1(a)

The relative contribution of the coupling term, $K_{12}\kappa/P$, to the axial behavior

b/L	$a/b = 0{\cdot}1$	$a/b = 0{\cdot}2$	$a/b = 0{\cdot}3$	$a/b = 0{\cdot}4$
0·1	$7{\cdot}38 \times 10^{-4}$	$3{\cdot}34 \times 10^{-3}$	$9{\cdot}15 \times 10^{-3}$	$2{\cdot}14 \times 10^{-2}$
0·04	$4{\cdot}86 \times 10^{-7}$	$2{\cdot}09 \times 10^{-6}$	$5{\cdot}18 \times 10^{-6}$	$1{\cdot}04 \times 10^{-5}$
0·02	$1{\cdot}91 \times 10^{-8}$	$8{\cdot}21 \times 10^{-8}$	$2{\cdot}02 \times 10^{-8}$	$3{\cdot}97 \times 10^{-8}$
0·01	$4{\cdot}49 \times 10^{-12}$	$3{\cdot}23 \times 10^{-11}$	$7{\cdot}97 \times 10^{-11}$	$1{\cdot}56 \times 10^{-10}$

TABLE 1(b)

The relative contribution of the coupling term, $K_{21}u_{,x}/M$, to the transverse behavior

b/L	$a/b = 0{\cdot}1$	$a/b = 0{\cdot}2$	$a/b = 0{\cdot}3$	$a/b = 0{\cdot}4$
0·1	$1{\cdot}99 \times 10^{-3}$	$7{\cdot}57 \times 10^{-3}$	$1{\cdot}67 \times 10^{-2}$	$2{\cdot}92 \times 10^{-2}$
0·04	$1{\cdot}32 \times 10^{-6}$	$4{\cdot}82 \times 10^{-6}$	$9{\cdot}73 \times 10^{-6}$	$1{\cdot}54 \times 10^{-5}$
0·02	$5{\cdot}20 \times 10^{-7}$	$1{\cdot}91 \times 10^{-7}$	$3{\cdot}84 \times 10^{-8}$	$6{\cdot}06 \times 10^{-8}$
0·01	$2{\cdot}05 \times 10^{-11}$	$7{\cdot}52 \times 10^{-11}$	$1{\cdot}53 \times 10^{-10}$	$2{\cdot}42 \times 10^{-10}$

The kinetic energy is given by

$$T = \frac{1}{2}\int_0^L \rho[(cv_{,x} + v_{,t})^2 + (c + cu_{,x} + u_{,t})^2]\,\mathrm{d}x, \tag{18}$$

where $\rho = \rho_0 - m\delta(x - x_0)$ is the mass per unit length of the beam, ρ_0 is the mass per unit length of the uncracked beam, m is the reduction in the mass per unit length occurring at the crack location, and c is the axial transport speed of the beam.

Using the expressions for the potential energy, kinetic energy, and mass conservation ($c\,\partial\rho/\partial x + \partial\rho/\partial t = 0$) with Hamilton's principle leads to the following uncoupled, linear partial differential equations which govern the unforced, undamped motion of a translating beam with an open crack:

$$\rho c^2 v_{,xx} + 2\rho c v_{,tx} + \rho v_{,tt} + (EIv_{,xx})_{,xx} - (Pv_{,x})_{,x} = 0, \tag{19}$$

$$\rho c^2 u_{,xx} + 2\rho c u_{,xt} + \rho u_{,tt} - \left[EA\left(u_{,x} + \frac{P}{EA}\right)\right]_{,x} = 0. \tag{20}$$

These equations are recast using the full expressions for EI and EA, and the following dimensionless quantities: a new spatial coordinate $\xi = x/L$, two new deformation coordinates $V = v/L$ and $U = u/L$, and a dimensionless time $\tau = t\sqrt{EI_0/\rho_0 L^4}$. The result is

$$(1 - \mu\delta)V_{,\tau\tau} + k_1(1 - \mu\delta)V_{,\xi\tau} + k_2(1 - \mu\delta)V_{,\xi\xi} - k_3(\delta_{,\xi\xi}V_{,\xi\xi} + 2\delta_{,\xi}V_{,\xi\xi\xi} - \delta V_{,\xi\xi\xi\xi}) + V_{,\xi\xi\xi\xi} - k_4 V_{\xi\xi} = 0, \tag{21}$$

$$(1 - \mu\delta)U_{,\tau\tau} + k_1(1 - \mu\delta)U_{,\xi\tau} + k_2(1 - \mu\delta)U_{,\xi\xi} + k_5[r\delta_{,\xi}U_{,\xi} - (1 - r\delta)U_{,\xi\xi}] = 0, \tag{22}$$

where $\mu = m/\rho_0, r = \Delta K_{11}L/EA_0, k_1 = 2c\sqrt{\rho_0 L^2/EI_0}, k_2 = \rho_0 L^2 c^2/EI_0, k_3 = \Delta K_{22}L/EI_0$, $k_4 = PL^2/EI_0$, $k_5 = A_0 L^2/I_0$. Furthermore, it should be understood that $\delta = \delta(\xi - \xi_0)$.

Spatial derivatives of $\delta(\xi - \xi_0)$ are evaluated using the technique described in reference [16].

2.5. NATURAL FREQUENCIES AND STABILITY

Having developed a model for a cracked, translating beam, the remainder of this work focuses on developing a fundamental understanding of the system's response characteristics. Specifically, the objective is to study the behavior of the linear natural frequencies and stability characteristics of the beam as the crack translates through the domain (between the supports).

To examine these characteristics, the governing equations are discretized using a Galerkin procedure with the expansions

$$U = \sum_{i=0}^{n} \alpha_i(\tau)\Psi_i(\xi), \qquad V = \sum_{i=0}^{n} \beta_i(\tau)\Phi_i(\xi), \tag{23}$$

where $\Psi_i(\xi) = \Phi_i(\xi) = \sin(i\pi\xi)$ for the simply supported boundary conditions under consideration here. These boundary conditions are justified by the fact that, in most applications, the axially moving material wraps around a pulley-type mechanism at the boundary—satisfying a no-slip condition between the beam and the pulley. This no-slip condition implies that the ends of the beam have no additional motion beyond the net translation which is common to the entire beam. Hence, the deformation fields U and V are zero at the ends.

The discretized equations may be written in matrix form as

$$[M]\ddot{\mathbf{x}} + [G]\dot{\mathbf{x}} + [K]\mathbf{x} = \mathbf{0}, \tag{24}$$

where $\mathbf{x} = \{\alpha_1, \alpha_2, \ldots, \beta_1, \beta_2, \ldots\}^t$, $[M]$ is the mass matrix, $[G]$ is the skew-symmetric gyroscopic matrix, and $[K]$ is the linear stiffness matrix. The natural frequencies for this system are found by rewriting equation (24) in first order form and solving the associated eigenvalue problem numerically [17].

3. RESULTS

3.1. TRANSVERSE VIBRATION

The model and the eigenvalue procedure developed in the previous sections are used to examine the influence of the crack on the dynamics and stability of the translating beam. Consider the transverse motion of a beam with a thickness-to-length ratio of $b/L = 0{\cdot}01$, a transport speed of half its critical speed $c/c_{cr} = 0{\cdot}5$, and a crack depth of $a/b = 0{\cdot}1$. This crack depth gives a mass loss ratio of $\mu = 0{\cdot}1$. The non-dimensional parameters are set to $k_1 = 3{\cdot}164$, $k_2 = 2{\cdot}503$, $k_3 = 2{\cdot}57 \times 10^{-3}$, $k_4 = 0{\cdot}151$, $k_5 = 1200$, $r = 1{\cdot}27 \times 10^{-9}$, and the critical speed is $c_{cr} = 33$ m/s. Figure 4(a) shows the imaginary part of the first and second eigenvalues as a function of the crack location for this case. As the crack enters the domain, the natural frequencies are those of the uncracked, translating beam (given by the dashed lines). As the crack translates to the right with the beam, there is a change in the frequencies. Both the first and the second mode frequencies begin to increase. The first mode frequencies continue to increase until a local maximum is achieved at the midspan and then they decrease monotonically until the crack exits the domain at $\xi_0 = 1$. The second mode eigenvalue locus experiences two local maxima and a local minimum.

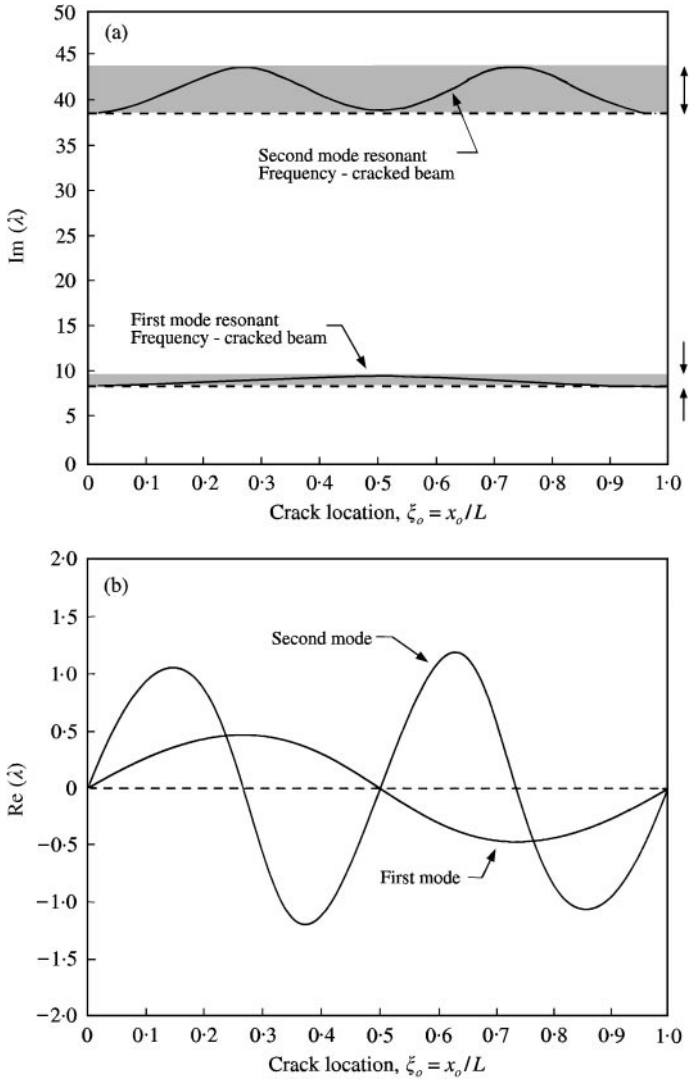

Figure 4. The (a) imaginary and (b) real parts of the transverse eigenvalue loci for the beam with a crack depth of $a/b = 0{\cdot}1$ and a transport speed of $c/c_{cr} = 0{\cdot}5$.

There are four important observations to be made regarding Figure 4(a). First, the frequencies are always larger than the uncracked travelling beam frequencies. This implies that for shallow cracks the decrease in the mass per unit length dominates the behavior (over the change in stiffness). This can be seen by noting that both the effective mass and stiffness decrease by the introduction of a crack in the beam. Since the frequency generally goes as $\sqrt{k_{eff}/m_{eff}}$ *and* the frequencies increase, the denominator must change more rapidly than the numerator, i.e., the change in the mass per unit length is the dominant feature of these shallow crack problems. Second, the $\mathrm{Im}(\lambda)$ loci are symmetric about the midspan $\xi_0 = 0{\cdot}5$. Third, the number of local maxima in each locus is equal to the mode number associated with that locus. Finally, the fluctuations of the natural frequencies have significant implications for the forced response. For a moment, consider the uncracked, translating beam. That system has an infinite but countable number of resonant frequencies

which should be avoided in the forced vibration problem. In the cracked beam problem, these resonant frequencies fluctuate, creating *frequency bands* associated with resonance in the cracked problem (these bands are darkened in the figure). If the system is excited at a frequency in one of these bands, the beam will begin to resonate as the natural frequency passes through the excitation frequency. Fortunately, a steady state resonance will not occur since the frequency continues to change. But a large transient may be initiated. Of course, the size of the transient depends on the transport speed which controls the duration that the natural frequency dwells near the excitation frequency.

The real parts of the eigenvalues are shown in Figure 4(b). When the crack initially enters the domain, $\mathrm{Re}(\lambda) = 0$. This is in agreement with the uncracked problem. As the crack begins to move through the domain all of the $\mathrm{Re}(\lambda_i)$ are positive, indicating the system is dynamically unstable. The stability of the first mode changes as the crack passes the midspan. The second mode locus fluctuates with a larger amplitude and twice the frequency of the first mode. Both loci return to zero as the crack exits the domain at $\xi_0 = 1$.

From Figure 4(b), it is evident that the $\mathrm{Re}(\lambda)$ loci are antisymmetric. As before, the number of local maxima is equal to the mode number. Finally, the system always destabilizes as the crack enters the domain (all $\mathrm{Re}(\lambda_i) > 0$). As the crack exits the domain, the system is always dynamically stable. The extent to which the system experiences unstable, growing transient oscillations depends on the transport speed. If the transport speed is low and the system lingers in an unstable region, a large amplitude oscillation will develop. However, if the transport speed is high, the crack will exit the dynamically unstable regime before a large amplitude response can develop.

Perhaps the most important revelation about this system is that both the natural frequencies and the dynamic stability characteristics change as the crack location (which can be viewed as a parameter) changes. But how do other parameters, such as the crack depth and the transport speed, influence the size of the resonant frequency bands? Figures 5(a) and 5(b) provide some insight. These show the size of the frequency bands as a function of the transport speed for crack depths of $a/b = 0{\cdot}1$ and $0{\cdot}3$, respectively. Comparing Figures 5(a) and 5(b) shows that deeper cracks lead to larger resonance bands for both modes (indeed, for all modes) at all transport speeds below c_{cr}. In both figures, the size of the first mode band does not change substantially for transport speeds below $c/c_{cr} = 0{\cdot}9$. As the divergence instability is approached at $c/c_{cr} = 1$, the upper boundary of the first mode resonance zone continues to decrease mildly but the lower boundary, associated with the frequency of the uncracked beam, drops to zero and widens the band. The second mode resonance becomes slightly more narrow with increases in the transport speed.

Finally, Figure 6 shows the complex eigenfunctions at various crack locations ($\xi_0 = 0{\cdot}2, 0{\cdot}5, 0{\cdot}8$) for the case $a/b = 0{\cdot}3$ and $c/c_{cr} = 0{\cdot}5$.

3.2. AXIAL VIBRATION

Axial vibrations are also influenced by the presence of an open crack. Figure 7(a) illustrates the behavior of the first two axial natural frequencies as the crack translates between the supports for the case $a/b = 0{\cdot}1$, $c/c_{cr} = 0{\cdot}5$, and the same set of constants given earlier.

Many of the trends discussed for transverse vibrations also hold here. The eigenvalue loci fluctuate and the number of maxima for a give locus equals the mode number, e.g., the first mode locus has one maximum. As the crack exits the span, the frequencies again return to those of the uncracked translating beam. The absolute magnitudes of the fluctuations in the

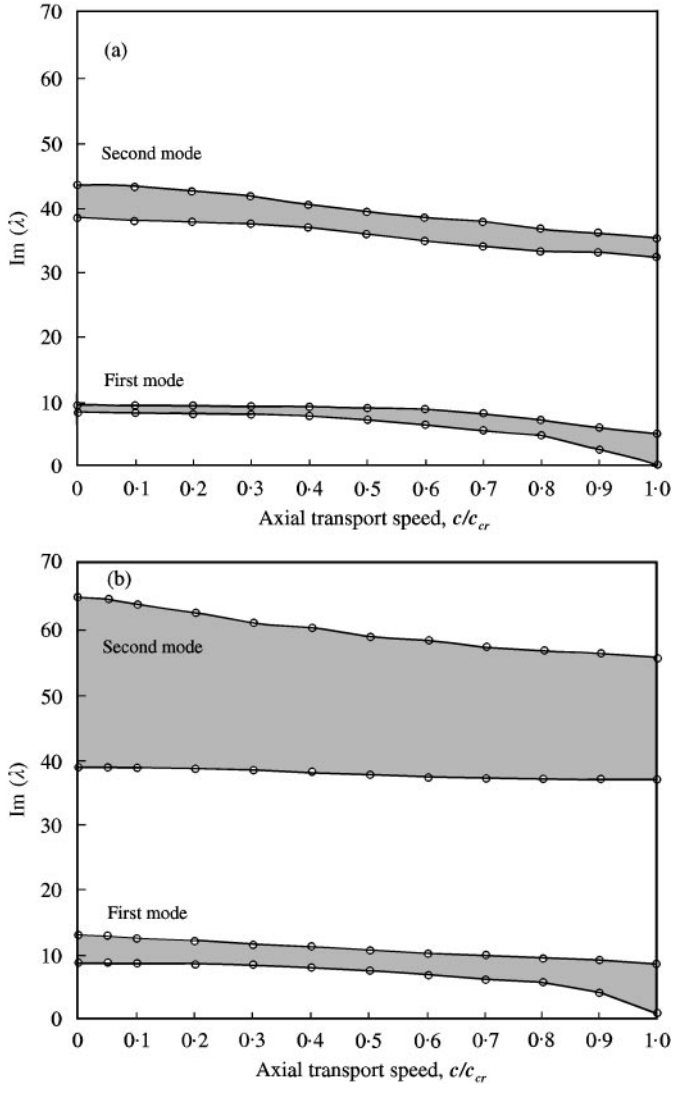

Figure 5. The resonance bands for transverse motion as a function of the transport speed for (a) a beam with a crack depth $a/b = 0{\cdot}1$ and (b) a beam with a crack depth$a/b = 0{\cdot}3$.

axial frequencies are much larger than those associated with transverse vibrations. However, relative to their respective frequency scales, there is parity. For example, the first and second *transverse* frequencies (see Figure 4(a)) experience up to 22 and 15% change from their nominal, uncracked values while the first and second axial frequencies experience up to 13 and 11% change. The real parts of the eigenvalues are presented in Figure 7(b). Again, the behavior is qualitatively similar to the results presented for transverse motion.

As before, the size of the resonance bands increase with mode number and crack depth. As the axial transport speed is increased, the axial resonance zones also shrink mildly. However, near the critical speed there is no drastic increase in the size of the first mode resonance band since the fundamental axial frequency is never reduced to zero.

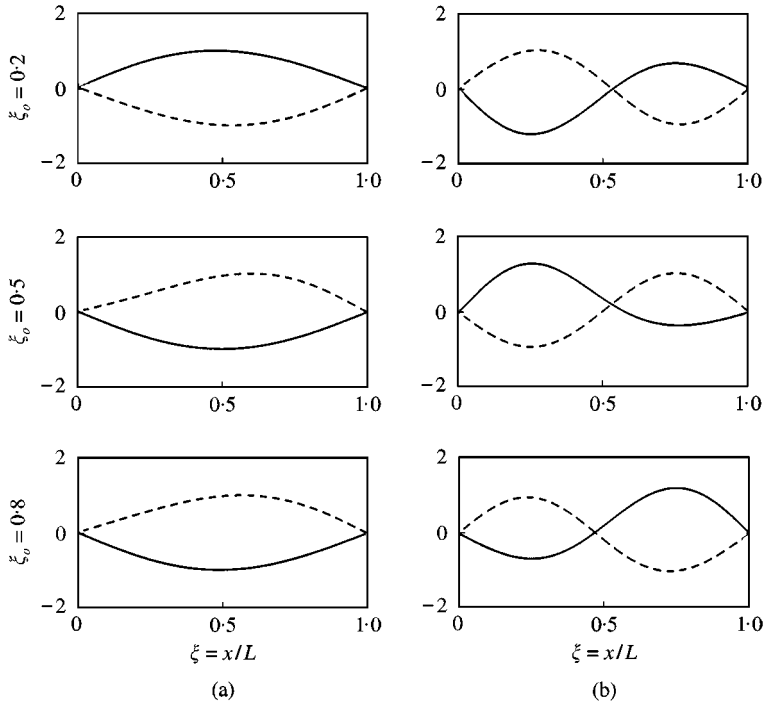

Figure 6. The real (- - - -) and imaginary (——) parts of the first two eigenvectors for three crack locations with $a/b = 0{\cdot}3$ and $c/c_{cr} = 0{\cdot}5$: (a) first mode, (b) second mode.

3.3. A BRIEF NOTE ON CONVERGENCE

During the discretization, the series presented in equations (23) were truncated to n terms. As a result, the issue of modal convergence arises. To ensure convergence of the first two eigenvalues, a convergence study was performed. This consisted of fixing the number of terms retained at n and computing the eigenvalues at four crack locations, $\xi_0 = 0{\cdot}2, 0{\cdot}4, 0{\cdot}6$, and $0{\cdot}8$. The value of n was increased and the eigenvalues were again computed. The eigenvalues were then plotted against the number of terms retained. Once the change in *all* of the eigenvalues was below 0·5%, the system was said to be converged. Typically, 10 terms ($n = 10$) were sufficient to ensure convergence of the transverse eigenvalues. The axial problem usually required many more modes to converge—usually in the range of $n = 24$.

4. CONCLUSIONS

The objective of this work is to study the dynamics of a translating beam containing an open crack. This problem is placed in a mathematical setting using linear elastic fracture mechanics to describe the global change in stiffness of the cracked beam. This change in stiffness and the discontinuity in the mass per unit length are localized in the vicinity of the crack using a delta function representation. In addition to describing the change in stiffness, fracture mechanics is also used to develop a loading criterion that signals the initiation of crack closure. Since an open crack is assumed, this criterion indicates the limitations of the vibration results which follow.

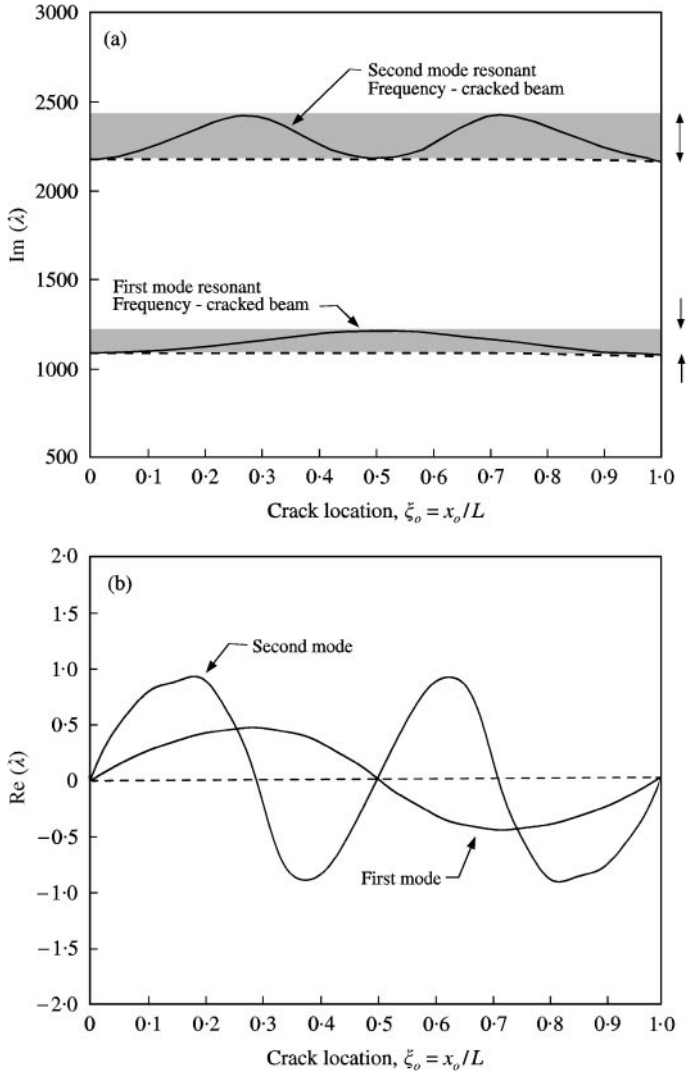

Figure 7. The (a) imaginary and (b) real parts of the axial eigenvalue loci for the beam with a crack depth of $a/b = 0{\cdot}1$ and a transport speed of $c/c_{cr} = 0{\cdot}5$.

Using the local change of stiffness, the equations governing the axial and transverse vibrations of a translating, cracked beam are developed using Hamilton's principle. These equations are non-dimensionalized and then discretized using a Galerkin projection. An eigenanalysis is then carried out to ascertain the behavior of the natural frequencies ($\mathrm{Im}(\lambda)$) and the dynamic stability characteristics ($\mathrm{Re}(\lambda)$).

It is shown that as the crack translates with the beam between the fixed end supports, the imaginary and real parts of the eigenvalues fluctuate. These fluctuations are seen as eigenvalue loci plotted as a function of crack location between $0 < \xi_0 < 1$. Turning to the natural frequencies first, these fluctuations imply that at a fixed excitation frequency in the resonance band the system will pass through resonance at least twice. This non-stationary problem could lead to large transient oscillations. The size of the resonance band increases

with mode number and crack depth. Furthermore, the size of each band is relatively insensitive to changes in the transport speed until approximately 90% of the first critical speed, at which time the first band widens in the transverse case.

As for the real part of the eigenvalues, each locus begins at zero and becomes positive. This indicates that the system is dynamically unstable and free oscillations will grow, albeit temporarily. As the crack continues to translate the loci fluctuate and all of the real parts become negative, though not simultaneously. This indicates that the motion is asymptotically stable.

In general, this work sheds light on some complexities in the modelling of axially translating beams possessing an open crack. It also demonstrates some of the fundamental, yet complicated, dynamics involved in this free vibration problem and alludes to some of the difficulties involved in the forced vibration problem.

ACKNOWLEDGMENT

The authors would like to thank Dr Matthew Begley for his many helpful discussions regarding fracture mechanics. The support of the National Science Foundation (grant no. CMS-9625319) is gratefully acknowledged.

REFERENCES

1. C. D. MOTE 1972 *Shock and Vibration Digest* **4**, 2–11. Dynamic stability of axially moving materials.
2. J. A. WICKERT and C. D. MOTE 1988 *Shock and Vibration Digest* **20**, 3–13. Current research on the vibration and stability of axially-moving materials.
3. M. CHATI, R. RAND and S. MUKHERJEE 1997 *Journal of Sound and Vibration* **207**, 249–270. Modal analysis of a cracked beam.
4. Y. C. CHU and M.-H. H. SHEN *AIAA Journal* **30**, 2512–2519. Analysis of forced bilinear oscillators and the application to cracked beam dynamics.
5. H. TADA, P. PARIS and G. IEWIN 1972 *The Stress Analysis of Cracks Handbook*. Hellertown, PA: Del Research Crop.
6. A. D. DIMAROGONAS 1996 *Engineering Fracture Mechanics* **55**, 831–857. Vibration of cracked structures: a state of the art review.
7. C. A. PAPADOPOULOS and A. D. DIMAROGONAS 1988 *Journal of Vibrations, Acoustics, Stress, and Reliability in Design* **110**, 1–8. Coupled longitudinal and bending vibrations of a cracked shaft.
8. A. D. DIMAROGONAS *et al.* 1983 *Journal of Sound and Vibration* **91**, 583–593. Vibration of cracked shafts in bending.
9. R. H. PLAUT, R. H. ANDRUET and S. SUTHERMAN 1994 *Journal of Sound and Vibration* **173**, 577–589. Behaviour of a cracked rotating shaft during passage through a critical speed.
10. A. S. SEKHAR 1999 *Journal of Sound and Vibration* **223**, 497–512. Vibration characteristics of a cracked rotor with two open cracks.
11. S. CHRISTIDES and A. D. S. BARR 1984 *International Journal of Mechanical Science* **26**, 639–648. One dimensional theory of cracked Euler–Bernoulli beams.
12. M.-H. H. SHEN and C. PIERRE 1990 *Journal of Sound and Vibration* **138**, 115–134. Natural modes of Bernoulli–Euler beams with symmetric cracks.
13. T. G. CHONDROS, A. D. DIMAROGONAS and J. YAO 1997 *Journal of Sound and Vibration* **200**, 303–313. A consistent cracked bar vibration theory.
14. J. A. WICKERT and C. D. MOTE Jr 1988 *Journal of the Acoustical Society* **84**, 963–969. Linear transverse vibration of axially moving string–particle system.
15. B. LAWN 1993 *Fracture of Brittle Solids*. Cambridge: Cambridge University Press, second edition.
16. D. J. COLWELL and J. R. GILLETT 1987 *International Journal of Mathematical Education in Science and Technology* **18**, 657–658. A property of the Dirac delta function.
17. L. MEIROVITCH 1980 *Computational Methods in Structural Dynamics*. The Netherlands: Noordhoff Publishing.

APPENDIX A: CHANGE IN COMPLIANCE DUE TO CRACK

To obtain the expressions for the change in compliance due to the presence of a crack, consider the beam shown in Figure A1(a), subjected to an axial load $P_1 = P$ and a bending moment $P_2 = M$. The resulting deformation consists of both axial deformation and an angular rotation. Let δ_{ij} represents the deformation ($i = 1$ for δ, $i = 2$ for θ) resulting from the application of P_j.

First, consider applying P_1 alone (i.e., $P_2 = 0$). The elastic strain energy stored in the beam is equal to the area under the load–deformation curve, shown in Figure A1(b): $U = \frac{1}{2} P_1 \delta_{11}$. Next, without unloading the structure, a bending moment P_2 is applied. This causes two new contributions to the strain energy—one from the angular displacement and another from an additional axial elongation induced by the bending moment, as shown in Figure A1(c). The total elastic strain energy becomes

$$U = \tfrac{1}{2} P_1 \delta_{11} + \tfrac{1}{2} P_2 \delta_{22} + \tfrac{1}{2} P_1 \delta_{12}.$$

Given the force–deformation relations, $\delta_{ij} = C_{ij} P_j$, the strain energy may be written as

$$U = \tfrac{1}{2} C_{11} P_1^2 + \tfrac{1}{2} C_{22} P_2^2 + \tfrac{1}{2} C_{12} P_1 P_2.$$

Now, if the loading sequence were reversed, the energy would be the same except for the final term. In this case, it would contain C_{21} rather than C_{12}. But, since the total energy must be the same regardless of the loading sequence, it is evident that $C_{12} = C_{21}$.

To evaluate these changes in compliance, the definition of the energy release rate is used. The energy release rate, G, is the strain energy released per unit crack area generated (by opening the crack), i.e., $G = -\,\mathrm{d}U/\mathrm{d}a$ for a crack of unit depth. Separating variables and using the expression for the strain energy leads to

$$\tfrac{1}{2} C_{11} P_1^2 + \tfrac{1}{2} C_{22} P_2^2 + C_{12} P_1 P_2 = \int_0^a G(\bar{a})\, \mathrm{d}\bar{a}.$$

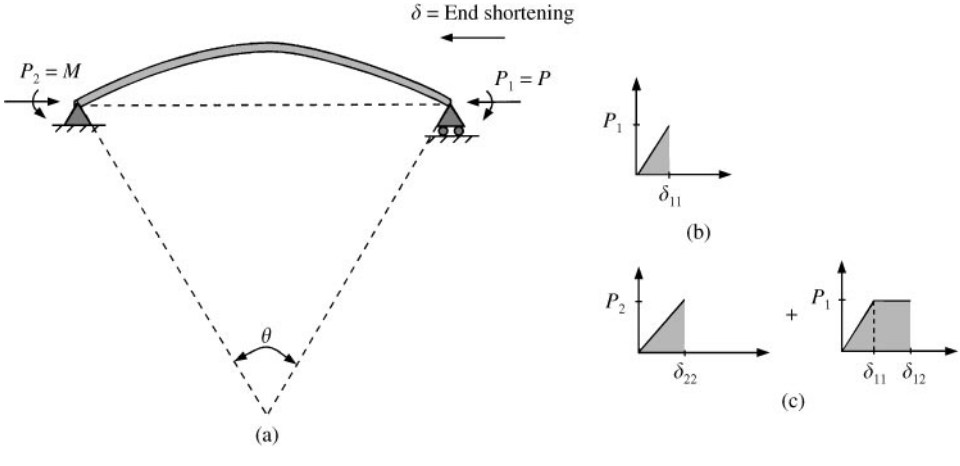

Figure A1. (a) The deformed beam described using the global co-ordinates d and θ. (b) The force–deformation curve and the stored energy for an applied axial load. (c) The force–deformation curve and the stored energy obtained by superimposing a bending moment on the system.

The compliance may then be expressed as

$$C_{ij} = \frac{\partial^2}{\partial P_i \partial P_j} \int_0^a G(\bar{a})\, \mathrm{d}\bar{a}.$$

Expressions for G are available in reference [5] for a variety of geometries.